IEEE Access
Multidisciplinary ⋮ Rapid Review ⋮ Open Access Journal

Received June 10, 2020, accepted June 27, 2020, date of publication June 30, 2020, date of current version July 20, 2020.

Digital Object Identifier 10.1109/ACCESS.2020.3006132

Current Prediction Error Reduction Method of Predictive Current Control for Permanent Magnet Synchronous Motors

FENG NIU[1], **(Member, IEEE), XIAOXIAO WANG**[1], **SHAOPO HUANG**[1], **XIAOYAN HUANG**[2], **(Member, IEEE), LIJIAN WU**[2], **(Senior Member, IEEE), KUI LI**[1], **AND YOUTONG FANG**[2], **(Senior Member, IEEE)**
[1]State Key Laboratory of Reliability and Intelligence of Electrical Equipment, Hebei University of Technology, Tianjin 300401, China
[2]College of Electrical Engineering, Zhejiang University, Hangzhou 310058, China

Corresponding author: Lijian Wu (ljw@zju.edu.cn)

This work was supported in part by the National Natural Science Foundation of China under Grant 51707174, and in part by the Natural Science Foundation of Hebei Province under Grant E2019202092.

ABSTRACT Predictive current control (PCC) has been widely investigated in motor drive field. The PCC is a model-based control method and the motor prediction model is quite sensitive to motor parameters which may be inaccurately measured and change under different working conditions. In order to reduce the current prediction error of PCC caused by inductance mismatch, a current prediction error reduction method is proposed for permanent magnet synchronous motor (PMSM) by online inductance correction which is based on the relationship between inductance mismatch and current prediction error. Firstly, a proportional regulator is used to obtain the absolute correction value according to the relationship between inductance error and current prediction error. Secondly, the polarity of correction value is judged according to the fluctuation amplitudes of predicted current and actual current. Finally, an adaptive adjustment method for correction period is proposed to ensure the accuracy of inductance correction value. Experimental tests are carried out to verify the effectiveness of proposed method, and results show that the proposed method can obviously reduce current prediction error and improve control performance in practical applications. In addition, the proposed method is suitable for interior and surface mounted PMSMs.

INDEX TERMS Current prediction error reduction, online inductance correction, permanent magnet synchronous motor (PMSM), predictive current control (PCC).

I. INTRODUCTION

Permanent magnet synchronous motor (PMSM) is widely used in industrial products and electric vehicles due to its high power density and simple structure [1]–[4]. In motor control field, predictive current control (PCC) has been widely investigated and applied. The PCC is a model-based control method and it is quite sensitive to motor parameters [5]–[9]. However, the motor parameters cannot be measured accurately in actual applications, and they may vary under different working conditions [10]. Mismatch of motor parameters is the main reason causing current prediction error of PCC, and it may result in inaccurate prediction of motor motion behavior [11], [12].

In order to solve the above problem, scholars have proposed many methods to reduce the prediction error, including prediction error compensation methods, motor parameter identification methods, model-free prediction algorithms and so on.

For prediction error compensation methods, in [13], by adding discrete time integral term to current prediction stage, a discrete-time robust PCC method is proposed to compensate current prediction error. In [14], the prediction errors provided by each voltage vector are added to current prediction stage with a weighting factor, which can effectively improve the prediction accuracy. The current prediction errors are various under different switching states [15], so, a variable weighting factor is presented in [16] based on the position and magnitude of reference voltage. Although the error compensation method can effectively reduce the prediction error, it does not solve the fundamental problem that causes prediction error.

Parameter mismatch is the primary cause of current prediction error, so, some studies have focused on motor

The associate editor coordinating the review of this manuscript and approving it for publication was Shihong Ding.

parameter identification, such as parameter offline identification algorithm and parameter online identification algorithm. Among them, the offline parameter identification algorithms are mostly implemented by using high frequency voltage injection methods [17], adding low-pass filters [18] and so on.

Online parameter identification methods include particle swarm optimization algorithm [19], [20], current injection method [21], [22], novel affine projection algorithm [23], mean square identification algorithm [24] and recursive algorithm [25]. There are also some algorithms that consider inverter disturbance voltage and take advantage of motor parameter difference in dynamics when implementing online multi-parameter identification [26], [27]. Besides, many published references have constructed various observers to achieve online parameter identification. In [28], the extended state observer is proposed to enhance inductance robustness and to compensate errors caused by stator inductance mismatch. Some sliding-mode observers are applied to obtain the motor parameters [29]–[31]. For example, in [30], [31], an adaptive-gain sliding mode observer is designed for sensorless control, which can automatically adjust the gain to adapt to actual working condition.

In order to reduce the disturbance caused by parameter mismatch, many scholars have constructed disturbance observers to simultaneously predict stator current and track system disturbance [32], [33]. In [34], the lumped disturbances caused by unknown load torque and parameter variations are derived, and a generalized proportional integral observer based on feed-forward compensated controller is proposed to estimate the flux and current for next step current prediction. In [35], an incremental prediction model is used to predict flux linkage and an inductance disturbance observer is proposed to update inductance value. In [36], a terminal sliding mode control based on nonlinear disturbance observer is proposed to compensate the parameter uncertainty and it realizes the tracking control of speed and current.

In order to eliminate the effect of motor parameter mismatch, many published references have developed the model-free predictive current control (MFPCC) algorithm. Unlike traditional model-based PCC, the MFPCC algorithm uses stator current difference between two switching states to achieve prediction without using any motor parameters [37]. However, the switching action inside inverter may cause current spikes. In order to solve this problem, scholars have proposed a method that the current detection is performed immediately before power device turns on or turns off in each sampling period [15], [38]. In [39], a weighting factor is added in prediction process to eliminate current spikes. The prediction accuracy can be enhanced by adjusting weighting factor. In MFPCC, prediction accuracy only depends on the measured current and current difference, which makes the current difference detection critical. To keep the current variation information up to date, scholars have made some improvements to MFPCC method. In [40], a current reconstruction algorithm is presented based on the relationship between voltage vectors. In [41], a continuous voltage vector MFPCC is proposed to reduce the current fluctuation, and the optimal voltage vector is obtained by online optimization of vector's phase and amplitude.

However, the MFPCC methods require a sufficiently short switching interval to ensure accuracy, which requires high hardware performance. And most of above mentioned parameter identification methods increase the computational burden of MPC, which makes control system more complex.

This paper aims to reduce the current prediction error of finite-control-set PCC strategy for PMSM, and improve the control performance of motor system. The main contributions of this paper are: a current prediction error reduction method based on online inductance correction is proposed, and it can directly correct the inductance value of prediction model only using one proportional regulator, which is simple and easy to implement. Compared with other methods, the proposed method can significantly reduce calculation burden, while the proposed method is suitable for both interior and surface mounted PMSMs. The paper is organized as follows. Section II presents the PMSM model and PCC algorithm, and the effect of parameter mismatch on current prediction error is analyzed. Based on the relationship between inductance error and current prediction error, the design of current prediction error reduction method is given in Section III. Section IV provides some experimental results to assess the performance of proposed method, and the paper is concluded in Section V.

II. PREDICTIVE CURRENT CONTROL

A. PMSM MODEL

The continuous state equations of PMSM in rotor reference frame are expressed as

$$\frac{\mathrm{d}i_\mathrm{d}}{\mathrm{d}t} = -\frac{R_\mathrm{s}}{L_\mathrm{d}}i_\mathrm{d} + \frac{\omega_\mathrm{e}L_\mathrm{q}}{L_\mathrm{d}}i_\mathrm{q} + \frac{1}{L_\mathrm{d}}u_\mathrm{d} \tag{1}$$

$$\frac{\mathrm{d}i_\mathrm{q}}{\mathrm{d}t} = -\frac{\omega_\mathrm{e}L_\mathrm{d}}{L_\mathrm{q}}i_\mathrm{d} - \frac{R_\mathrm{s}}{L_\mathrm{q}}i_\mathrm{q} + \frac{1}{L_\mathrm{q}}u_\mathrm{q} - \frac{\omega_\mathrm{e}\psi_\mathrm{f}}{L_\mathrm{q}} \tag{2}$$

where i_d and i_q are d- and q-axes stator currents, u_d and u_q are d- and q-axes stator voltages, L_d and L_q are d- and q-axes inductances, R_s is stator resistance, ω_e and ψ_f are rotor electrical angular speed and flux linkage of permanent magnet, respectively. In order to predict d- and q-axes stator current for next sampling instant, the continuous state equations in (1) and (2) need to be discretized by the forward Euler approximation method. The discrete prediction model of PMSM is obtained as follows

$$i_\mathrm{d}^\mathrm{p}(k+1) = i_\mathrm{d}(k) - \frac{T_\mathrm{s}R_\mathrm{s}i_\mathrm{d}(k)}{L_\mathrm{d}} + \frac{T_\mathrm{s}\omega_\mathrm{e}L_\mathrm{q}i_\mathrm{q}(k)}{L_\mathrm{d}} + \frac{T_\mathrm{s}u_\mathrm{d}(k)}{L_\mathrm{d}} \tag{3}$$

$$i_\mathrm{q}^\mathrm{p}(k+1) = i_\mathrm{q}(k) - \frac{T_\mathrm{s}R_\mathrm{s}i_\mathrm{q}(k)}{L_\mathrm{q}} - \frac{T_\mathrm{s}\omega_\mathrm{e}L_\mathrm{d}i_\mathrm{d}(k)}{L_\mathrm{q}} + \frac{T_\mathrm{s}u_\mathrm{q}(k)}{L_\mathrm{q}} - \frac{T_\mathrm{s}\omega_\mathrm{e}\psi_\mathrm{f}}{L_\mathrm{q}} \tag{4}$$

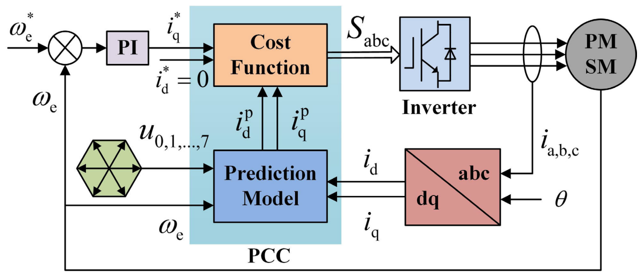

FIGURE 1. Block diagram of PCC for PMSM.

where the superscript p represents prediction value, T_s is the control period, $X(k)$ $(k = 1, 2, 3, \ldots)$ is the value of X at time kT_s and X represents predicted and actual values of d- and q-axis currents.

B. PREDICTIVE CURRENT CONTROL

The block diagram of PCC scheme for PMSM is shown in Fig. 1. For a two-level three-phase voltage-source inverter, there are eight switching states, which can provide eight voltage vectors including two zero vectors and six active vectors. The future states of motor system under these eight voltage vectors are predicted according to (3) and (4). Then, the prediction results are evaluated to select the optimal voltage vector according to cost function (CF) which is expressed as

$$CF = \left|i_d^p(k+1) - i_d^*(k+1)\right|^2 + \left|i_q^p(k+1) - i_q^*(k+1)\right|^2 \quad (5)$$

where the superscript * represents reference values. The voltage vector which can minimize CF is chosen as the optimal one and corresponding switching signals will drive inverter in next control period.

C. EFFECT OF PARAMETER MISMATCH ON PREDICTION ERROR

The PCC is sensitive to motor parameters, and the accuracy of model parameters will directly influence control performance of motor system. In actual applications, the motor parameters cannot be measured accurately, and they may change due to temperature, saturation effect and other environmental effects. For example, temperature increase will cause the increase of resistance and the decrease of permanent magnet flux linkage. The d- and q-axes inductances may vary due to magnetic saturation [21], [22]. The effect of model parameter mismatch on current prediction error of PCC is analyzed in this section. In this work, the current prediction error (PE) is defined as the difference between predicted value and actual value of d- and q-axes current, which is expressed as

$$PE = i_x^p(k+1) - i_x^a(k+1), \quad x \in \{d,q\} \quad (6)$$

where the superscript p represents predicted current values and superscript a represents actual current values.

In the PMSM prediction model, the d- and q-axes inductance, stator resistance and flux linkage are L_{dm}, L_{qm}, R_m and ψ_{fm}, respectively. According to (3) and (4), the current prediction model can be expressed as

$$i_d^p(k+1) = i_d(k) - \frac{T_s R_m i_d(k)}{L_{dm}} + \frac{T_s \omega_e L_{qm} i_q(k)}{L_{dm}} + \frac{T_s u_d(k)}{L_{dm}} \quad (7)$$

$$\begin{aligned} i_q^p(k+1) = {} & i_q(k) - \frac{T_s R_m i_q(k)}{L_{qm}} - \frac{T_s \omega_e L_{dm} i_d(k)}{L_{qm}} + \frac{T_s u_q(k)}{L_{qm}} \\ & - \frac{T_s \omega_e \psi_{fm}}{L_{qm}}. \end{aligned} \quad (8)$$

For the actual motor, the d- and q-axes inductance, stator resistance and flux linkage are $L_{da} = L_{dm} + \Delta L_d$, $L_{qa} = L_{qm} + \Delta L_q$, $R_a = R_m + \Delta R$, and $\psi_{fa} = \psi_{fm} + \Delta\psi$, respectively, where ΔL_d, ΔL_q, ΔR, and $\Delta\psi$ are deviations between actual values and values in prediction model. So, actual current can be calculated by

$$\begin{aligned} i_d^a(k+1) &= i_d(k) - \frac{T_s R_a}{L_{da}} i_d(k) + \frac{T_s \omega_e L_{qa}}{L_{da}} i_q(k) + \frac{T_s}{L_{da}} u_d(k) \\ &= i_d(k) - \frac{T_s (R_m + \Delta R)}{L_{dm} + \Delta L_d} i_d(k) + \frac{T_s}{L_{dm} + \Delta L_d} u_d(k) \\ &\quad + \frac{T_s \omega_e \left(L_{qm} + \Delta L_q\right)}{L_{dm} + \Delta L_d} i_q(k) \end{aligned} \quad (9)$$

$$\begin{aligned} i_q^a(k+1) &= i_q(k) - \frac{T_s R_a}{L_{qa}} i_q(k) - \frac{T_s \omega_e L_{da}}{L_{qa}} i_d(k) + \frac{T_s u_q(k)}{L_{qa}} \\ &\quad - \frac{T_s \omega_e \psi_{fa}}{L_{qa}} \\ &= i_q(k) - \frac{T_s (R_m + \Delta R)}{L_{qm} + \Delta L_q} i_q(k) + \frac{T_s}{L_{qm} + \Delta L_q} u_q(k) \\ &\quad - \frac{T_s \omega_e \left(L_{dm} + \Delta L_d\right)}{L_{qm} + \Delta L_q} i_d(k) - \frac{T_s \omega_e (\psi_{fm} + \Delta\psi)}{L_{qm} + \Delta L_q}. \end{aligned} \quad (10)$$

According to (6)-(10), the current prediction errors of d- and q-axis, namely PE_i_d and PE_i_q, can be obtained

$$\begin{aligned} PE\_i_d = {} & \frac{\Delta R L_{dm} - R_m \Delta L_d}{L_{dm}\left(L_{dm} + \Delta L_d\right)} T_s i_d(k) + \frac{\Delta L_d T_s u_d(k)}{L_{dm}\left(L_{dm} + \Delta L_d\right)} \\ & + \frac{\Delta L_d L_{qm} - \Delta L_q L_{dm}}{L_{dm}\left(L_{dm} + \Delta L_d\right)} T_s \omega_e i_q(k) \end{aligned} \quad (11)$$

$$\begin{aligned} PE\_i_q = {} & \frac{\Delta R L_{qm} - R_m \Delta L_q}{L_{qm}\left(L_{qm} + \Delta L_q\right)} T_s i_q(k) + \frac{\Delta L_q T_s u_q(k)}{L_{qm}\left(L_{qm} + \Delta L_q\right)} \\ & + \frac{\Delta L_d L_{qm} - \Delta L_q L_{dm}}{L_{qm}\left(L_{qm} + \Delta L_q\right)} T_s \omega_e i_d(k) \\ & + \frac{\Delta\psi L_{qm} - \psi_{fm} \Delta L_q}{L_{qm}\left(L_{qm} + \Delta L_q\right)} T_s \omega_e. \end{aligned} \quad (12)$$

It can be obviously seen from (11) and (12) that the mismatch of any motor parameter will lead to current prediction error. According to existing literature, stator inductance mismatch has the greatest effect on current prediction error [11]. It can be observed from (11) and (12) that the effect of resistance deviation ΔR is only reflected in first part of (11) and (12), and prediction errors are proportional to ΔR. The magnetic flux deviation $\Delta\psi$ only affects PE_i_q, and PE_i_q is proportional to $\Delta\psi$. The inductance deviation has an effect on each part of (11) and (12), which is more complicated

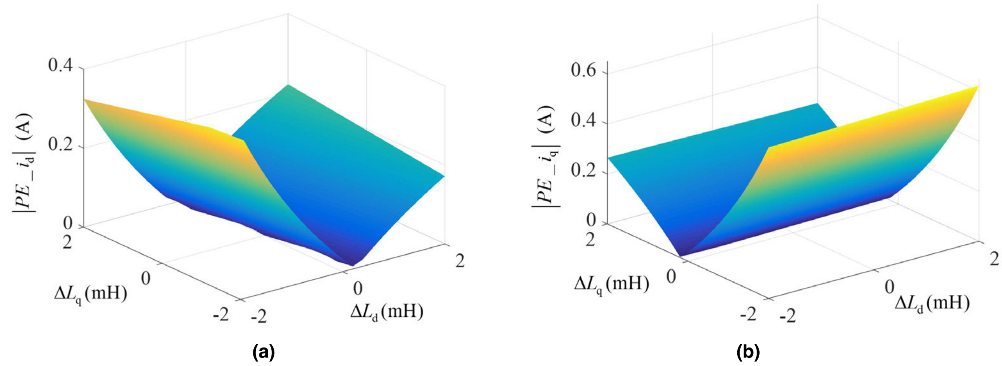

FIGURE 2. The absolute prediction error values under various mismatch degree of inductance parameters. (a) Relationship between absolute value of d-axis current prediction error and mismatch degree of d- and q-axes inductance values. (b) Relationship between absolute value of q-axis current prediction error and mismatch degree of d- and q-axes inductance values.

than that caused by other parameter mismatch. In this paper, the effect of inductance deviations on prediction errors are mainly considered.

To further analyze the impact of ΔL_d and ΔL_q on current prediction errors, the graphical illustrations of absolute current prediction error value with various mismatch degrees of L_d and L_q are shown in Fig. 2 under the working condition of 1 Nm load and 1000 r/min. It can be seen that ΔL_d can influence PE_i_d more obviously and same relationship also exists between ΔL_q and PE_i_q. Besides, the effect of negative deviations of stator inductance is more obvious.

III. CURRENT PREDICTION ERROR REDUCTION METHOD

Based on the inherent relationship between parameter mismatch and prediction error, the prediction error feedback mechanism is introduced to realize online correction of prediction model parameter. In this section, the design of current prediction error reduction method based on online inductance correction is detailed illustrated.

A. RELATIONSHIP BETWEEN PREDICTION ERROR AND INDUCTANCE MISMATCH

The model predictive control is a nonlinear control scheme, which leads to a complex mapping relationship between prediction error and parameter mismatch. According to the analysis in last section, the current prediction errors are mostly affected by stator inductance mismatch. Therefore, the current prediction error reduction method proposed in this paper is based on the relationship between current prediction error and inductance parameter mismatch.

For interior PMSM (IPMSM) with different L_d and L_q, the d- and q-axes inductance deviations are defined as $\Delta L_d = L_{da}$-L_{dm} and $\Delta L_q = L_{qa}$-L_{qm}, respectively, where the subscript m represents inductance values in motor prediction model and subscript a represents actual inductance values. Then the current prediction errors of d- and q-axis can be obtained

$$PE\_i_d = \frac{\Delta L_d T_s}{L_{dm}\left(L_{dm}+\Delta L_d\right)}\mathrm{A_d} + \frac{\Delta L_d L_{qm} - \Delta L_q L_{dm}}{L_{dm}(L_{dm}+\Delta L_d)}\mathrm{B_d} \quad (13)$$

$$PE\_i_q = \frac{\Delta L_q T_s}{L_{qm}\left(L_{qm}+\Delta L_q\right)}\mathrm{A_q} + \frac{\Delta L_d L_{qm} - \Delta L_q L_{dm}}{L_{qm}\left(L_{qm}+\Delta L_q\right)}\mathrm{B_q} \quad (14)$$

where $\mathrm{A_d} = -R_s i_d(k) + u_d(k)$, $\mathrm{A_q} = -R_s i_q(k) + u_q(k) - \psi_f\omega_e$, $\mathrm{B_d} = T_s\omega_e i_q(k)$ and $\mathrm{B_q} = T_s\omega_e i_d(k)$. Solving (13) and (14), the relationships between inductance deviations and current prediction errors can be obtained as follow

$$\Delta L_d = \frac{-\mathrm{B_1A_2} + \mathrm{C_1B_2}}{\mathrm{A_1A_2} + \mathrm{C_1C_2}} \quad (15)$$

$$\Delta L_q = -\frac{\mathrm{B_2}}{\mathrm{A_2}} + \frac{\mathrm{C_2}}{\mathrm{A_2}}\frac{-\mathrm{B_1A_2} + \mathrm{C_1B_2}}{\mathrm{A_1A_2} + \mathrm{C_1C_2}} \quad (16)$$

where

$$\begin{cases} \mathrm{A_1} = PE\_i_d \times L_{dm} - \mathrm{A_d}T_s - L_{qm}\mathrm{B_d} \\ \mathrm{B_1} = PE\_i_d \times L_{dm}^2 \\ \mathrm{C_1} = L_{dm}\mathrm{B_d} \end{cases} \quad (17)$$

$$\begin{cases} \mathrm{A_2} = PE\_i_q \times L_{qm} - \mathrm{A_q}T_s + L_{dm}\mathrm{B_q} \\ \mathrm{B_2} = PE\_i_q \times L_{qm}^2 \\ \mathrm{C_2} = L_{qm}\mathrm{B_q}. \end{cases} \quad (18)$$

For (17) and (18), the orders of magnitude of $\mathrm{A_x}$, $\mathrm{B_x}$ and $\mathrm{C_x}$ ($x \epsilon \{1, 2\}$) are 10^{-2}, 10^{-7} and 10^{-6}, respectively. Then comparing the magnitude of each part of (15) and (16), and ignoring the smaller parts, the approximate relationship between inductance deviation and prediction error can be obtained

$$\begin{aligned} \Delta L_d &\approx -\frac{\mathrm{B_1}}{\mathrm{A_1}} \\ &= \frac{-PE\_i_d \times L_{dm}^2}{PE\_i_d L_{dm} + \left(R_s i_d(k) + u_d(k) - L_{qm}\omega_e i_q(k)\right) T_s} \end{aligned} \quad (19)$$

$$\begin{aligned} \Delta L_q &\approx -\frac{\mathrm{B_2}}{\mathrm{A_2}} \\ &= \frac{-PE\_i_q \times L_{qm}^2}{PE\_i_q L_{qm} + (R_s i_q(k) - u_q(k) + \psi_f\omega_e + L_{dm}\omega_e i_d(k))T_s}. \end{aligned} \quad (20)$$

For the denominator of (19), the order of magnitude of $PE\_i_d \times L_{dm}$ is 10^{-4}, and the order of magnitude of rest part is 10^{-2}. Therefore, the influence of $PE\_i_d \times L_{dm}$ in (19) can be ignored. The case of (20) is similar to (19). Then by simplifying (19) and (20), the absolute values of inductance deviations can be obtained

$$|\Delta L_{\rm d}| \approx \left| \frac{L_{\rm dm}^2}{\left(R_{\rm s} i_{\rm d}(k) + u_{\rm d}(k) - L_{\rm qm}\omega_{\rm e} i_{\rm q}(k)\right) T_{\rm s}} \right| \times |PE\_i_{\rm d}| \quad (21)$$

$$|\Delta L_{\rm q}| \approx \left| \frac{L_{\rm qm}^2}{(R_{\rm s} i_{\rm q}(k) - u_{\rm q}(k) + \psi_{\rm f}\omega_{\rm e} + L_{\rm dm}\omega_{\rm e} i_{\rm d}(k)) T_{\rm s}} \right| \times |PE\_i_{\rm q}|. \quad (22)$$

According to (21) and (22), there exists a proportional relationship between the absolute values of inductance deviations and that of current prediction errors.

Surface mounted PMSM (SPMSM, $L_{\rm d} = L_{\rm q}$) can be seen as a special case of IPMSM. In SPMSM control system, the $i_{\rm d} = 0$ control is mostly used in practical applications, which makes the prediction error of q-axis current more obvious than that of d-axis. Therefore, the relationship between q-axis current prediction error and stator inductance parameter mismatch is mainly considered. For actual SPMSM, stator inductance is $L_{\rm a}$. The stator inductance of SPMSM prediction model is $L_{\rm m}$. Then $PE\_i_{\rm q}$ can be shown as

$$PE\_i_{\rm q} = \frac{L_{\rm m} - L_{\rm a}}{L_{\rm m} L_{\rm a}} \left[R_{\rm s} i_{\rm q}(k) + \omega_{\rm e}\psi_{\rm f} - u_{\rm q}(k)\right] T_{\rm s}. \quad (23)$$

The stator inductance error ΔL is defined as $\Delta L = L_{\rm a} - L_{\rm m}$, and the relationship between ΔL and $PE\_i_{\rm q}$ is obtained as follows

$$\Delta L = \frac{-PE\_i_{\rm q} \times L_{\rm m}^2}{PE\_i_{\rm q} \times L_{\rm m} + \left[R_{\rm s} i_{\rm q}(k) + \omega_{\rm e}\psi_{\rm f} - u_{\rm q}(k)\right] T_{\rm s}}. \quad (24)$$

For the denominator of (24), the order of magnitude of $PE\_i_{\rm q} \times L_{\rm m}$ is 10^{-4} and the order of magnitude of rest part is 10^{-2}. Therefore, the influence of $PE\_i_{\rm q} \times L_{\rm m}$ in (24) can be ignored and the absolute value of ΔL can be obtained

$$|\Delta L| \approx \left| \frac{L_{\rm m}^2}{\left[R_{\rm s} i_{\rm q}(k) + \omega_{\rm e}\psi_{\rm f} - u_{\rm q}(k)\right] T_{\rm s}} \right| \times \left|PE\_i_{\rm q}\right|. \quad (25)$$

According to (25), there exists a proportional relationship between $|\Delta L|$ and $|PE\_i_{\rm q}|$. So, the inductance online feedback correction can be realized through a proportional regulator. The input signal of proportional regulator is current prediction error, and the output signal is the absolute correction value of inductance parameter, while the order of magnitude of proportional coefficient is from 10^{-4} to 10^{-3} according to (25). In practical applications, the initial gain value of proportional regulator can be obtained by (25), and then fine tune the value according to different operating conditions.

B. INDUCTANCE ERROR POLARITY

In the last section, the absolute correction value of inductance parameter is obtained, and in this section, the polarity of correction value is judged according to the fluctuation amplitude of predicted current and actual current.

According to (7) and (8), the fluctuation amplitude of predicted current is inversely proportional to the polarity of inductance deviation. For example, if the inductance value in prediction model is greater than the actual value, the fluctuation amplitude of predicted current will be smaller than that of actual current. On the contrary, the fluctuation amplitude of predicted current will be larger than that of actual current. Based on the above conclusion, the polarity of absolute correction value can be judged by

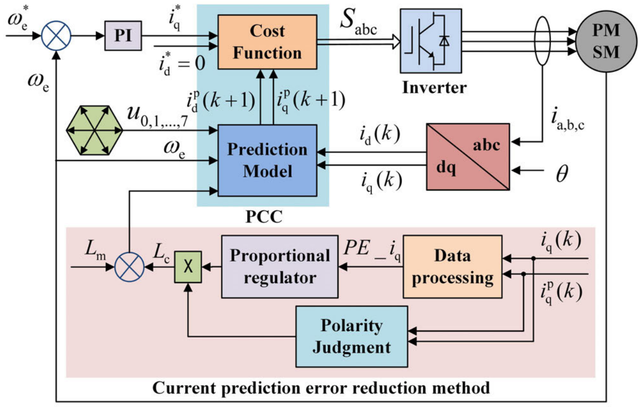

FIGURE 3. Block diagram of current prediction error reduction method.

$$\begin{cases} \text{negative}, \sum \left|i_{\rm q}^{\rm p}(k) - \text{mean}\left(i_{\rm q}^{\rm p}(k)\right)\right| \\ \qquad < \sum \left|i_{\rm q}(k) - \text{mean}\left(i_{\rm q}(k)\right)\right| \\ \text{positive}, \sum \left|i_{\rm q}^{\rm p}(k) - \text{mean}\left(i_{\rm q}^{\rm p}(k)\right)\right| \\ \qquad > \sum \left|i_{\rm q}(k) - \text{mean}\left(i_{\rm q}(k)\right)\right| \end{cases} \quad (26)$$

where mean(X) is the average value of current over a data window period $T_{\rm d}$. The data window period $T_{\rm d}$ is related to inductance correction period $T_{\rm c}$, which will be illustrated in the next section.

According to the absolute correction value and inductance error polarity, inductance correction value $L_{\rm c}$ can be calculated, and the block diagram of current prediction error reduction method is shown in Fig. 3.

C. CORRECTION PERIOD

According to the test results, the current prediction errors vary periodically and the variation period of prediction error changes under different motor speed. The higher the motor speed is, the shorter the variation period of current prediction error is. So, the determination of inductance correction period will affect the effectiveness of proposed method. If the correction period is too long, the inductance error cannot be corrected in time. Conversely, if the correction period is too short, the correction period cannot contain enough current prediction error variation periods, which may lead to the wrong correction value and its polarity according to (25) and (26). In addition, too frequent corrections may cause system instability.

Because the variation period of current prediction error is related to motor rotation speed, this paper proposes a correction period automatic adjustment method, in which the inductance correction period can be adaptively adjusted according to the motor speed. The principle of this method

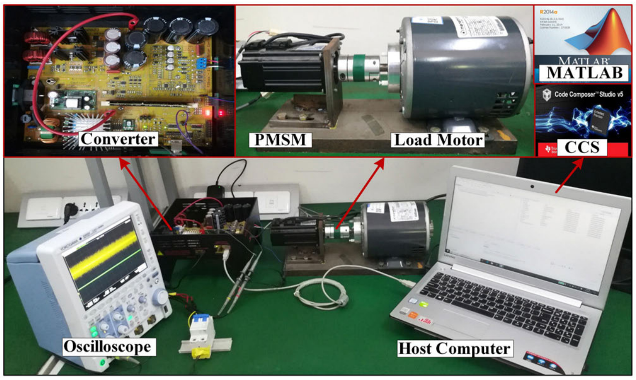

FIGURE 4. The experimental platform.

TABLE 1. Parameters of motor control system.

Symbol	Quantity	Value	Unit
P_n	rated power	400	W
I_n	rated current	2.8	A
ω_n	rated speed	3000	r/min
T_n	rated torque	1.27	Nm
R_s	stator resistance	2.35	Ω
L_s	stator inductance	6.5	mH
ψ_f	permanent magnet flux linkage	0.0755	Wb
n_p	number of pole pairs	4	pairs
U_{dc}	DC bus voltage	200	V
T_s	control period	100	μs

can be expressed by

$$T_c = T_d = \frac{2\pi n_p}{\omega_e} \times 20, \tag{27}$$

where n_p is the number of pole pairs. In (27), the inductance correction period T_c is equal to data window period T_d, and both of them contain fixed number of mechanical rotation cycles (fixed number of current prediction error periods).

IV. EXPERIMENTAL VERIFICATION

In order to verify the effectiveness of proposed current prediction error reduction method, the experimental platform is implemented as shown in Fig. 4, and the main parameters of motor control system are shown in Table 1. The PCC model is established using MATLAB/Simulink to generate C code, and the PCC algorithm is implemented using DSP TMS320F28335 processor.

In the experiment, the inductance value given by motor manufacturer L_s is regarded as actual inductance, and the inductance deviation is artificially designed by setting different inductance values in prediction model of PCC.

The experimental results of current prediction error reduction method are shown in Fig. 5(a) and Fig. 5(b). The waveforms from top to bottom are stator inductance of motor prediction model L_m, prediction errors of q- and d-axes currents, electromagnetic torque T_e and flux linkage ψ_s, respectively. The results are obtained under the conditions of 40% inductance parameter mismatch ($L_m = 9.1$ mH, $L_s = 6.5$ mH), and the motor speed is 1500 r/min while load torque $T_L = 1.27$ Nm in Fig. 5(a) and no load in Fig. 5(b). It can be obviously seen that the proposed method can effectively correct the inductance value in motor prediction model, and the system control performance are improved. Under the condition of $T_L = 1.27$ Nm, after the proposed method is utilized, the PE_i_q and PE_i_d are reduced by 20.18% and 5.13%, respectively, and torque ripple T_{rip} and flux ripple ψ_{rip} are reduced by 30.13% and 48.01%, respectively. Similar results can be obtained under the condition of no load.

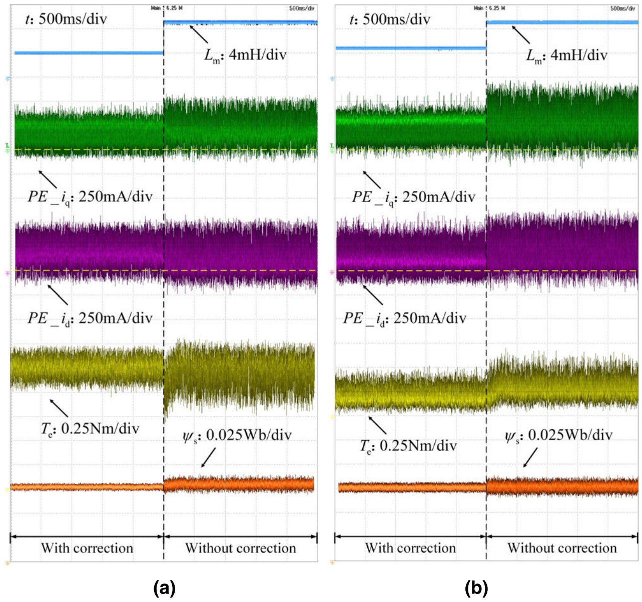

FIGURE 5. The experimental results of proposed method with 40% inductance mismatch ($L_m = 9.1$ mH, $L_s = 6.5$ mH). (a) Under 1.27 Nm load and 1500 r/min. (b) Under no load and 1500 r/min.

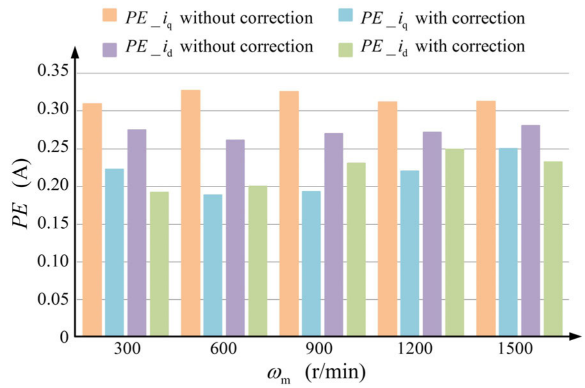

FIGURE 6. The results of d- and q-axes current prediction errors with 40% inductance mismatch ($L_m = 9.1$ mH, $L_s = 6.5$ mH) under different speeds.

Fig. 6 shows the results of d- and q-axes current prediction errors with 40% inductance mismatch in cases where $T_L = 1.27$ Nm and ω_m is changed from 300 r/min to 1500 r/min by the step of 300 r/min. Fig. 7 shows the results of torque ripple T_{rip} and flux ripple ψ_{rip}. The results show

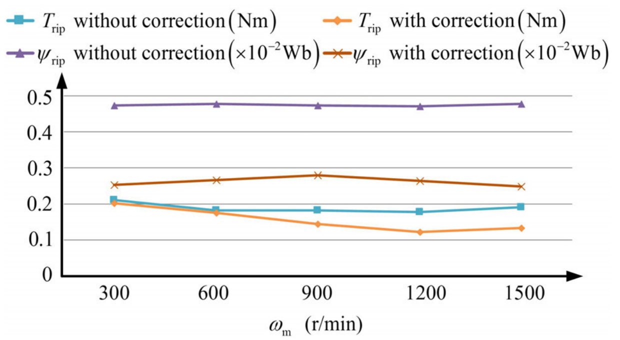

FIGURE 7. The results of torque ripple T_{rip} and flux ripple ψ_{rip} with 40% inductance mismatch under different speeds.

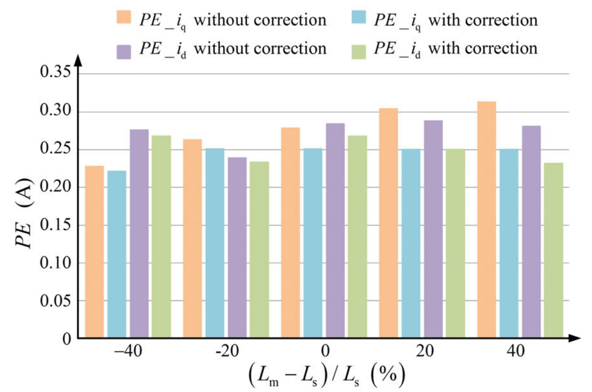

FIGURE 8. The results of d- and q-axes current prediction errors with different inductance mismatch degrees under 1.27 Nm load and 1500 r/min.

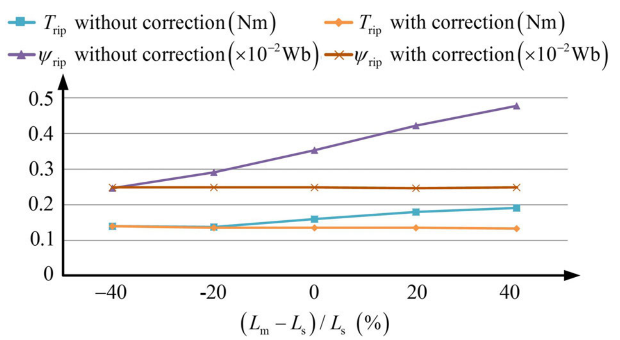

FIGURE 9. The results of torque ripple T_{rip} and flux ripple ψ_{rip} with different inductance mismatch degrees under 1.27 Nm load and 1500 r/min.

that the proposed method can significantly reduce current prediction errors under different speeds, while the control performance can be improved.

Fig. 8 shows the results of d- and q-axes current prediction errors in cases where $T_L = 1.27$ Nm, $\omega_m = 1500$ r/min and inductance mismatch is changed from -40% to 40% by the step of 20%. Fig. 9 shows the results of torque ripple T_{rip} and flux ripple ψ_{rip}. Table 2 shows the numerical results of current prediction error reduction and control performance. The results show that the proposed method can achieve significant reduction of current prediction error under different inductance mismatch degrees, while the control performance can be improved.

TABLE 2. Results under different inductance mismatch (%).

(%)

$(L_m$-$L_s)/L_s$	-40	-20	0	20	40
Reduction percentage of PE_i_q	2.96	4.43	9.59	17.61	20.18
Reduction percentage of PE_i_d	2.91	2.64	5.60	13.06	17.58
Reduction percentage of T_{rip}	-0.64	1.45	14.28	23.67	30.13
Reduction percentage of ψ_{rip}	-1.14	14.21	29.62	41.79	48.01

TABLE 3. Correction results of inductance.

$(L_m$-$L_s)/L_s$ (%)	-40	-20	0	20	40
L_m (mH)	3.9	5.2	6.5	7.8	9.1
L_m with correction (mH)	4.14	4.12	4.14	4.13	4.13

Table 3 shows the inductance values after correction under different inductance mismatch degrees. Two points need to be noted in the table: 1. In the case of no inductance mismatch, the proposed method still corrects inductance parameters to reduce prediction error. 2. The inductance value is corrected to approximately 4.13 mH for different mismatch degrees, while the inductance value given by motor manufacturer L_s is 6.5 mH. The reasons are as follows: 1. The inductance value provided by motor manufacturer L_s is a nominal value, but actual inductance value may vary during different operation conditions, resulting in a difference between actual and nominal inductance value. For example, magnetic saturation effect may lead to the result that actual inductance value is smaller than the given value. 2. Except inductance mismatch, the current prediction error may be caused by many other factors, such as resistance and magnetic flux mismatch, prediction step size, discretization order of motor prediction model and so on. Therefore, the influence of other factors on prediction error will be reflected in inductance correction value, and the corrected inductance value may differ from given value. The objective of proposed method is reducing prediction error and improving control performance, but not obtaining accurate inductance value.

Besides, the dynamic response of proposed method is fast during the experiments. The correction response is related to the proportional coefficient of regulator and correction period, which can be improved by increasing proportional coefficient and shortening correction period. However, large proportional coefficient will result in the oscillation of corrected inductance value, and short correction period will cause system instability. In the experiment, these two parameters can be fine-tuned according to (25) and (27) to give full play of proposed method.

V. CONCLUSION

In this paper, a current prediction error reduction method of PCC for PMSM based on online inductance correction is proposed and it has been experimentally applied to a SPMSM system. The major conclusions of this paper include: 1. The mismatch of motor parameters can lead to current prediction errors, and the deviation of stator inductance is the most important factor causing current prediction error. 2. For $i_d = 0$ control of SPMSM, there exists a proportional relationship between inductance deviation and q-axis current prediction error, and the polarity of inductance deviation is opposite to the current prediction error. 3. The current prediction errors vary periodically and the variation period changes according to motor speed. 4. Experimental results show that the proposed method can achieve significant reduction of current prediction error, while the control performance can be improved. 5. The current prediction error reduction method based on online inductance correction is suitable for both IPMSM and SPMSM. Compared to other similar methods, the proposed method is simple and easy to implement in practical applications. Besides, it should be noted that current prediction error is difficult to completely eliminate, and the objective of proposed method is to reduce current prediction error as much as possible rather than eliminate it completely.

REFERENCES

[1] F. Niu, B. Wang, A. S. Babel, K. Li, and E. G. Strangas, "Comparative evaluation of direct torque control strategies for permanent magnet synchronous machines," *IEEE Trans. Power Electron.*, vol. 31, no. 2, pp. 1408–1424, Feb. 2016.

[2] Q. Hou, S. Ding, and X. Yu, "Composite super-twisting sliding mode control design for PMSM speed regulation problem based on a novel disturbance observer," *IEEE Trans. Energy Convers.*, early access, Apr. 6, 2020, doi: 10.1109/TEC.2020.2985054.

[3] Y. Miao, H. Ge, M. Preindl, J. Ye, B. Cheng, and A. Emadi, "MTPA fitting and torque estimation technique based on a new flux-linkage model for interior-permanent-magnet synchronous machines," *IEEE Trans. Ind. Appl.*, vol. 53, no. 6, pp. 5451–5460, Nov. 2017.

[4] S. Cao, F. Niu, X. Huang, S. Huang, Y. Wang, K. Li, and Y. Fang, "Time–frequency characteristics research of common mode current in PWM motor system," *IEEE Trans. Power Electron.*, vol. 35, no. 2, pp. 1450–1458, Feb. 2020.

[5] M. Preindl and S. Bolognani, "Model predictive direct speed control with finite control set of PMSM drive systems," *IEEE Trans. Power Electron.*, vol. 28, no. 2, pp. 1007–1015, Feb. 2013.

[6] Y. Jiang, W. Xu, C. Mu, and Y. Liu, "Improved deadbeat predictive current control combined sliding mode strategy for PMSM drive system," *IEEE Trans. Veh. Technol.*, vol. 67, no. 1, pp. 251–263, Jan. 2018.

[7] F. Niu, X. Huang, L. Ge, J. Zhang, L. Wu, Y. Wang, K. Li, and Y. Fang, "A simple and practical duty cycle modulated direct torque control for permanent magnet synchronous motors," *IEEE Trans. Power Electron.*, vol. 34, no. 2, pp. 1572–1579, Feb. 2019.

[8] L. Wu, H. Yin, D. Wang, and Y. Fang, "A nonlinear subdomain and magnetic circuit hybrid model for open-circuit field prediction in surface-mounted PM machines," *IEEE Trans. Energy Convers.*, vol. 34, no. 3, pp. 1485–1495, Sep. 2019.

[9] X. Zhang and B. Hou, "Double vectors model predictive torque control without weighting factor based on voltage tracking error," *IEEE Trans. Power Electron.*, vol. 33, no. 3, pp. 2368–2380, Mar. 2018.

[10] C. Lai, G. Feng, K. Mukherjee, and N. C. Kar, "Investigations of the influence of PMSM parameter variations in optimal stator current design for torque ripple minimization," *IEEE Trans. Energy Convers.*, vol. 32, no. 3, pp. 1052–1062, Sep. 2017.

[11] J. Li, X. Huang, F. Niu, C. You, L. Wu, and Y. Fang, "Prediction error analysis of finite-control-Set model predictive current control for IPMSMs," *Energies*, vol. 11, no. 8, p. 2051, Aug. 2018.

[12] H. A. Young, M. A. Perez, and J. Rodriguez, "Analysis of finite-control-set model predictive current control with model parameter mismatch in a three-phase inverter," *IEEE Trans. Ind. Electron.*, vol. 63, no. 5, pp. 3100–3107, May 2016.

[13] T. Turker, U. Buyukkeles, and A. F. Bakan, "A robust predictive current controller for PMSM drives," *IEEE Trans. Ind. Electron.*, vol. 63, no. 6, pp. 3906–3914, Jun. 2016.

[14] M. Siami, D. A. Khaburi, A. Abbaszadeh, and J. Rodriguez, "Robustness improvement of predictive current control using prediction error correction for permanent-magnet synchronous machines," *IEEE Trans. Ind. Electron.*, vol. 63, no. 6, pp. 3458–3466, Jun. 2016.

[15] C.-K. Lin, T.-H. Liu, J.-T. Yu, L.-C. Fu, and C.-F. Hsiao, "Model-free predictive current control for interior permanent-magnet synchronous motor drives based on current difference detection technique," *IEEE Trans. Ind. Electron.*, vol. 61, no. 2, pp. 667–681, Feb. 2014.

[16] A. Abbaszadeh, D. A. Khaburi, H. Mahmoudi, and J. Rodríguez, "Simplified model predictive control with variable weighting factor for current ripple reduction," *IET Power Electron.*, vol. 10, no. 10, pp. 1165–1174, Aug. 2017.

[17] G. Wang, Y. Wang, J. Qi, R. Ni, W. Chen, and D. Xu, "Offline inductance identification of PMSM with adaptive inverter nonlinearity compensation," in *Proc. 9th Int. Conf. Power Electron. ECCE Asia (ICPE-ECCE Asia)*, Jun. 2015, pp. 2438–2444.

[18] H. Zhang, W. Wu, and L. Wang, "An improved off-line identification technology for parameters of surface permanent magnet synchronous motors," in *Proc. 20th Int. Conf. Electr. Mach. Syst. (ICEMS)*, Aug. 2017, pp. 1–4.

[19] O. Sandre-Hernandez, R. Morales-Caporal, J. Rangel-Magdaleno, H. Peregrina-Barreto, and J. N. Hernandez-Perez, "Parameter identification of PMSMs using experimental measurements and a PSO algorithm," *IEEE Trans. Instrum. Meas.*, vol. 64, no. 8, pp. 2146–2154, Aug. 2015.

[20] Z.-H. Liu, H.-L. Wei, Q.-C. Zhong, K. Liu, X.-S. Xiao, and L.-H. Wu, "Parameter estimation for VSI-fed PMSM based on a dynamic PSO with learning strategies," *IEEE Trans. Power Electron.*, vol. 32, no. 4, pp. 3154–3165, Apr. 2017.

[21] G. Feng, C. Lai, and N. C. Kar, "A novel current injection-based online parameter estimation method for PMSMs considering magnetic saturation," *IEEE Trans. Magn.*, vol. 52, no. 7, pp. 1–4, Jul. 2016.

[22] G. Feng, C. Lai, K. Mukherjee, and N. C. Kar, "Current injection-based online parameter and VSI nonlinearity estimation for PMSM drives using current and voltage DC components," *IEEE Trans. Transport. Electrific.*, vol. 2, no. 2, pp. 119–128, Jun. 2016.

[23] M. S. Rafaq, F. Mwasilu, J. Kim, H. H. Choi, and J.-W. Jung, "Online parameter identification for model-based sensorless control of interior permanent magnet synchronous machine," *IEEE Trans. Power Electron.*, vol. 32, no. 6, pp. 4631–4643, Jun. 2017.

[24] J. Sawma, F. Khatounian, E. Monmasson, L. Idkhajine, and R. Ghosn, "Analysis of the impact of online identification on model predictive current control applied to permanent magnet synchronous motors," *IET Electr. Power Appl.*, vol. 11, no. 5, pp. 864–873, May 2017.

[25] Z. Chen, J. Qiu, and M. Jin, "Adaptive finite-control-set model predictive current control for IPMSM drives with inductance variation," *IET Electr. Power Appl.*, vol. 11, no. 5, pp. 874–884, May 2017.

[26] W. Deng, C. Xia, Y. Yan, Q. Geng, and T. Shi, "Online multiparameter identification of surface-mounted PMSM considering inverter disturbance voltage," *IEEE Trans. Energy Convers.*, vol. 32, no. 1, pp. 202–212, Mar. 2017.

[27] D. Q. Dang, M. S. Rafaq, H. H. Choi, and J.-W. Jung, "Online parameter estimation technique for adaptive control applications of interior PM synchronous motor drives," *IEEE Trans. Ind. Electron.*, vol. 63, no. 3, pp. 1438–1449, Mar. 2016.

[28] M. Yang, X. Lang, J. Long, and D. Xu, "Flux immunity robust predictive current control with incremental model and extended state observer for PMSM drive," *IEEE Trans. Power Electron.*, vol. 32, no. 12, pp. 9267–9279, Dec. 2017.

[29] X. Zhang and Z. Li, "Sliding-mode observer-based mechanical parameter estimation for permanent magnet synchronous motor," *IEEE Trans. Power Electron.*, vol. 31, no. 8, pp. 5732–5745, Aug. 2016.

[30] C. Yang, T. Ma, Z. Che, and L. Zhou, "An adaptive-gain sliding mode observer for sensorless control of permanent magnet linear synchronous motors," *IEEE Access*, vol. 6, pp. 3469–3478, 2018.

[31] E.-K. Kim, J. Kim, H. T. Nguyen, H. H. Choi, and J.-W. Jung, "Compensation of parameter uncertainty using an adaptive sliding mode control strategy for an interior permanent magnet synchronous motor drive," *IEEE Access*, vol. 7, pp. 11913–11923, 2019.

[32] X. Zhang, B. Hou, and Y. Mei, "Deadbeat predictive current control of permanent-magnet synchronous motors with stator current and disturbance observer," *IEEE Trans. Power Electron.*, vol. 32, no. 5, pp. 3818–3834, May 2017.

[33] J. Ren, Y. Ye, G. Xu, Q. Zhao, and M. Zhu, "Uncertainty-and-disturbance-estimator-based current control scheme for PMSM drives with a simple parameter tuning algorithm," *IEEE Trans. Power Electron.*, vol. 32, no. 7, pp. 5712–5722, Jul. 2017.

[34] J. Wang, F. Wang, G. Wang, S. Li, and L. Yu, "Generalized proportional integral observer based robust finite control set predictive current control for induction motor systems with time-varying disturbances," *IEEE Trans. Ind. Informat.*, vol. 14, no. 9, pp. 4159–4168, Sep. 2018.

[35] X. Zhang, L. Zhang, and Y. Zhang, "Model predictive current control for PMSM drives with parameter robustness improvement," *IEEE Trans. Power Electron.*, vol. 34, no. 2, pp. 1645–1657, Feb. 2019.

[36] X. Liu, H. Yu, J. Yu, and L. Zhao, "Combined speed and current terminal sliding mode control with nonlinear disturbance observer for PMSM drive," *IEEE Access*, vol. 6, pp. 29594–29601, 2018.

[37] C.-K. Lin, J.-T. Yu, Y.-S. Lai, and H.-C. Yu, "Improved model-free predictive current control for synchronous reluctance motor drives," *IEEE Trans. Ind. Electron.*, vol. 63, no. 6, pp. 3942–3953, Jun. 2016.

[38] M. S. Mubarok and T.-H. Liu, "Implementation of predictive controllers for matrix-converter-based interior permanent magnet synchronous motor position control systems," *IEEE J. Emerg. Sel. Topics Power Electron.*, vol. 7, no. 1, pp. 261–273, Mar. 2019.

[39] Y. Zhang and J. Liu, "An improved model-free predictive current control of PWM rectifiers," in *Proc. 20th Int. Conf. Electr. Mach. Syst. (ICEMS)*, Aug. 2017, pp. 1–5.

[40] P. G. Carlet, F. Tinazzi, S. Bolognani, and M. Zigliotto, "An effective model-free predictive current control for synchronous reluctance motor drives," *IEEE Trans. Ind. Appl.*, vol. 55, no. 4, pp. 3781–3790, Jul. 2019.

[41] Y. Zhou, H. Li, R. Liu, and J. Mao, "Continuous voltage vector model-free predictive current control of surface mounted permanent magnet synchronous motor," *IEEE Trans. Energy Convers.*, vol. 34, no. 2, pp. 899–908, Jun. 2019.

FENG NIU (Member, IEEE) was born in Hebei, China, in 1986. He received the B.S and Ph.D. degrees from the Hebei University of Technology, Tianjin, China, in 2009 and 2015, respectively, all in electrical engineering.

From 2012 to 2014, he was a Research Fellow with the Electrical Machines and Drives Laboratory, Michigan State University, East Lansing, MI, USA. From 2016 to 2018, he was a Postdoctoral Research Fellow with the College of Electrical Engineering, Zhejiang University, Hangzhou, China. He is currently a Professor with the School of Electrical Engineering, Hebei University of Technology. He has authored or coauthored over 40 technical articles. His current research interests include motor system and control, and intelligent electrical equipment.

XIAOXIAO WANG was born in Hebei, China, in 1996. She received the B.S. degree in electrical engineering and automation from the Xi'an University of Technology, Shaanxi, China, in 2017. She is currently pursuing the M.S. degree in electrical engineering with the Hebei University of Technology, Tianjin, China.

Her current research interests include motor system and control.

SHAOPO HUANG was born in Xingtai, China, in 1986. He received the B.S. and M.S. degrees in electrical engineering from the Hebei University of Technology, Tianjin, China, in 2009 and 2012, respectively, where he is currently pursuing the Ph.D. degree in electrical engineering.

From 2017 to 2019, he was a Research Fellow with the Electrical Machines and Drives Laboratory, Michigan State University, East Lansing, MI, USA. His current research interests include reliability and life prediction of electrical apparatus and fault diagnosis of motor.

XIAOYAN HUANG (Member, IEEE) received the B.E. degree in control measurement techniques and instrumentation from Zhejiang University, Hangzhou, China, in 2003, and the Ph.D. degree in electrical machines and drives from the University of Nottingham, Nottingham, U.K., in 2008.

From 2008 to 2009, she was a Research Fellow with the University of Nottingham. She is currently a Professor with the College of Electrical Engineering, Zhejiang University, where she is working on electrical machines and drives. Her research interests include PM machines and drives for aerospace and traction applications, and generator systems for urban networks.

LIJIAN WU (Senior Member, IEEE) received the B.Eng. and M.Sc. degrees from the Hefei University of Technology, Hefei, China, in 2001 and 2004, respectively, and the Ph.D. degree from the University of Sheffield, Sheffield, U. K., in 2011, all in electrical engineering.

From 2004 to 2007, he was an Engineer with Delta Electronics Company, Ltd., Shanghai, China. From 2012 to 2013, he was with the Sheffield Siemens Wind Power Research Center, Sheffield, as a Design Engineer focusing on wind power generators. From 2013 to 2016, he was an Advanced Engineer with Siemens Wind Power A/S, Brande, Denmark. Since 2016, he has been working with Zhejiang University, Hangzhou, China, where he is currently working as a Professor of electrical machines and control systems. His current major research interests include design and control of permanent magnet machines.

KUI LI was born in Baoding, China, in 1965. He received the B.S. and M.S. degrees in electrical engineering from the Hebei University of Technology, Tianjin, China, in 1987 and 1992, respectively, and the Ph.D. degree in electrical engineering from Fuzhou University, Fuzhou, China, in 1996.

He is currently a Professor with the School of Electrical Engineering, Hebei University of Technology. He has authored or coauthored over 100 technical articles and two monographs. His current research interests include reliability and intellectualization of electrical apparatus, fault diagnosis, and life prediction of electrical apparatus.

YOUTONG FANG (Senior Member, IEEE) received the B.S. and Ph.D. degrees in electrical engineering from the Hebei University of Technology, Hebei, China, in 1984 and 2001, respectively.

He is currently a Professor with the College of Electrical Engineering, Zhejiang University, Hangzhou, China. His research interests include the application, control, and design of electrical machines.